ARMA 16-120

SAND2016-1617C

Laboratory Testing of Surrogate Non-degraded Waste Isolation Pilot Plant Materials

Broome, S.T., Ingraham, M.D., Flint, G.M., Hileman, M.B., Barrow, P.C.
Geomechanics Department, Sandia National Laboratories, Albuquerque, NM, USA
Herrick, C.G.
Performance Assessment and Decision Analysis Department, Sandia National Laboratories, Carlsbad, NM, USA

This paper was prepared for presentation at the 50th US Rock Mechanics / Geomechanics Symposium held in Houston, TX, USA, 26–29 June 2016. This paper was selected for presentation at the symposium by an ARMA Technical Program Committee based on a technical and critical review of the paper by a minimum of two technical reviewers. The material, as presented, does not necessarily reflect any position of ARMA, its officers, or members. Electronic reproduction, distribution, or storage of any part of this paper for commercial purposes without the written consent of ARMA is prohibited. Permission to reproduce in print is restricted to an abstract of not more than 300 words; illustrations may not be copied. The abstract must contain conspicuous acknowledgement of where and by whom the paper was presented

ABSTRACT: The present study results are focused on laboratory testing of surrogate materials representing WIPP waste. The surrogate wastes correspond to a conservative estimate of the containers and TRU waste materials emplaced at the WIPP. Testing consists of hydrostatic, triaxial, and uniaxial tests performed on surrogate waste recipes based on those previously developed by Hansen et al. (1997). These recipes represent actual waste by weight percent of each constituent and total density. Testing was performed on full-scale and ¼-scale containers. Axial, lateral, and volumetric strain and axial and lateral stress measurements were made. Unique testing techniques were developed during the course of the experimental program. The first involves the use of a spirometer to measure sample volumetric strain under the various stress conditions. Since the manner in which the waste containers deformed when compressed was not even, the volumetric and axial strains were used to determine the lateral strains. The second technique involved the development of unique coating procedures that also acted as jackets during hydrostatic, triaxial and full-scale uniaxial testing; ¼-scale uniaxial tests were not coated but wrapped with clay to maintain an airtight seal for volumetric strain measurement. During all testing methods, the coatings allowed the use of either a spirometer or precision flow meter to estimate the amount of air driven from the container as it crushed down since the jacket adhered to the container and yet was flexible enough to remain airtight during deformation.

1. INTRODUCTION

The Waste Isolation Pilot Plant (WIPP) is a United States (US) Department of Energy (DOE) mined, underground repository, certified by the US Environmental Protection Agency (EPA), and designed for the safe management, storage, and disposal of transuranic (TRU) radioactive waste resulting from the US defense programs. The wastes are emplaced in panels excavated at a depth of 655 m (2,150 ft) in the Permian Salado Formation. Following emplacement of waste and the engineered barrier material MgO, the panels will be isolated from the operational mine using an approved closure system. The repository is linked to the surface by four shafts that ultimately will be decommissioned and sealed.

Performance Assessment (PA) modeling of WIPP performance requires full and accurate understanding of coupled mechanical, hydrological, and geochemical processes and how they evolve through time. The overarching objective of this paper focuses on room closure modeling, specifically the compaction behavior of waste and obtaining a well-designed data set to parameterize an improved waste constitutive model. Ultimately, changes in the room closure model or other elements of the underground evolution will require acceptance by the EPA typically through a peer review process.

Research was undertaken in 1988 (Butcher et al., 1991) to determine the response of simulated waste and full-scale waste packages under emplacement conditions. An important conclusion of these studies was that the response of 55 gallon prototype waste drums undergoing moderate amounts of deformation is well characterized in ¼-scale experiments using No. 12 food cans (Baker et al., 1980) to simulate the waste packages. Even though some differences were noted in the lip-closure configurations, the lid and drum wall thickness, and the yield and ultimate strengths of the food cans versus the waste drums (Huerta et al., 1983 and Baker et al., 1980), the investigators concluded that the ¼-scale tests appeared to provide all the information needed to perform valid simulations.

Additional compaction studies (VandeKraats, 1987 and Wawersik, 2001) were conducted with crushed salt backfill packed around the cans. Since the current emplacement method does not include backfill around the waste packages, it is anticipated that early deformation resulting from disposal room back and floor closure will occur with little confinement until the ribs close sufficiently to contact the packages. Therefore, some of the currently available data generated with backfill may be used better for validation of a particular waste model than directly in determining parameters for the model. In addition, in the previous studies only axial load – axial deformation measurements or lateral load – lateral deformation measurements were made on either the ¼-scale or the full-scale tests. No hydrostatic or triaxial tests were performed. Thus, it is not possible to distinguish between uniaxial compression along the major axis of the waste drum and confined compaction, where only lateral stresses are present. This lack of multi-axial data, led modelers to adopt an isotropic, volumetric plasticity approach that can provide good predictability under unconfined conditions, but not under multi-axial states of stress and has resulted in some observed non-physical behavior of the material model. The multi-axial tests performed in the current study will provide a more complete data set for modeling.

The specific objectives of this study are to perform hydrostatic, uniaxial, and triaxial compression tests on ¼-scale waste packages filled with a recipe representative of current baseline inventory to allow for the determination of a complete set of waste constitutive model parameters. Quarter-scale testing is convenient for this task since the Sandia National Laboratories Geomechanics laboratory has available all axial loading and pressure equipment that can accommodate simulated waste packages of this size. For these tests, both axial displacements and total volume changes were measured to fill in data that were not generated by previous experiments. Assuming the deformations are approximately axisymmetric, all three principal components of stress and deformation can be determined as the waste package is compacted.

In addition to ¼-scale tests, full-scale hydrostatic and uniaxial loading tests were performed to validate the scaling assumptions and provide a basis for evaluating the performance of the waste constitutive model in predicting the compressive behavior of standard waste package systems. These were carried out following evaluation of the results of the ¼-scale tests.

This paper documents hydrostatic, uniaxial, and triaxial (¼-scale) and hydrostatic and uniaxial (55 gallon drum or full-scale) compaction tests conducted on surrogate non-degraded waste.

2. MATERIAL AND SAMPLE PREPARATION

The surrogate waste recipe used in this study was developed based on material proportions from Hansen et al (1997) and the density from the CRA-2014 inventory estimate. The weight percent values are in good agreement with the inventory estimates used in the most recent recertification application for WIPP (CRA-2014) and have been accepted by the EPA for several other WIPP model parameters determinations. By their nature, inventory estimates vary slightly from year to year. The sample density used for all tests in the current study (0.5055 g/cc) matches that of CRA-2014 to better represent the average density of drums received for emplacement in the WIPP repository. A description of the constituents used for both ¼- and full-scale samples is presented in Table 1.

Once the constituents were prepared as outlined in Table 1, they were combined into either the ¼-scale #12 food can or a 55 gallon drum (Figure 1). For all samples, a piece of felt metal was placed on the inside of the lid over the vent port to ensure the vent port did not get clogged during compaction of the waste. Once the container was loaded with surrogate waste, it was sealed with either an industrial food can sealer or, in the case of full scale specimens, a ring clamp was tightened to create an air tight seal. As will be discussed in the following sections, an air tight seal is critical to the measurement techniques employed.

Table 1: Ingredient description for recipe developed from Hansen et al. (1997) and CRA-2014.

Percent by weight of materials in test specimens	
Material	Weight Percent
Metals (iron, steel container, aluminum, copper)	52.0%
Cellulosics (pine wood and rags)	7.1%
Rubber and Plastics (latex gloves, polyethylene bottles and pipe, drum liner)	9.2%
Sorbents (portland cement and oilsorb)	4.1%
Sludges (glass, Hydrostone®, organic absorption resin, cement, soil)	27.5%
Total batch size	100%

Fig. 1. A) ¼-scale (#12 food can with 15.7 cm rim diameter) and B) full-scale (55 gallon drum with 60.6 cm rim diameter) containers loaded with surrogate waste ready for lid installation. C) full-scale sample with surrogate waste ready for loading into container.

The sealed samples were then jacketed with material to prevent confining fluid from infiltrating the sample and, in the case of uniaxial tests, keep the can sealed to ensure volume strain measurements are collected for the duration of the test. Because a lengthy trial and error process was performed to establish the most reliable jacketing method for each test type, it is worth further discussion here.

For the uniaxial ¼-scale samples, initially no jacket was used for the first portion of the test. After a pre-determined amount of compaction or a pause in response in air flow exiting the can (indicating a breach in the can), the test was paused and the sample was covered with modeling clay. As shown in Figure 2, a balloon was then rolled over the clay and taped to the top and bottom testing platens ensuring an airtight seal. The clay and balloon jacketing technique was used on the ¼-scale tests because the ¼-scale cans would frequently split along the side wall during compaction and the resulting large hole needed to be kept air tight. The motivation for an airtight seal will be discussed further in sections 3 and 4.

Fig. 2. A) ¼-scale uniaxial test before jacketing and B) after clay and balloon jacketing.

Uniaxial full-scale tests did not split along the side as frequently as ¼-scale tests. Therefore, full-scale uniaxial samples were coated with PMC®-770 urethane rubber prior to testing (Figure 3). This coating remains very flexible when dry and had a negligible effect on the strength of the sample during uniaxial compaction.

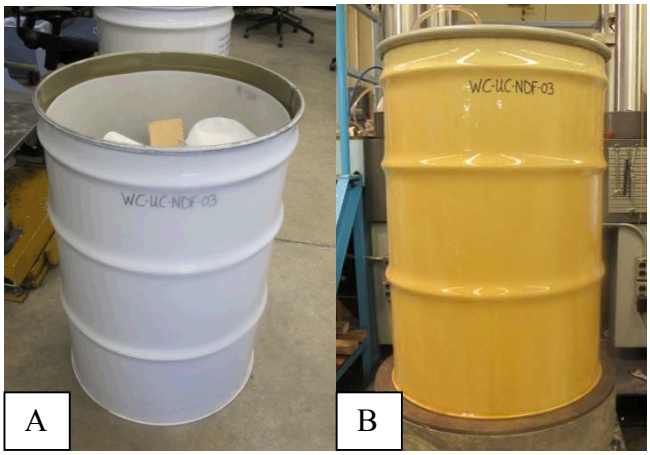

Fig. 3. A) full scale uniaxial sample before jacketing without lid and ring clamp and B) after urethane rubber jacketing.

The jacketing technique developed for hydrostatic and triaxial ¼-scale samples was more complicated than the uniaxial tests. The first two ¼-scale hydrostatic tests were jacketed with three layers of blue Loctite SF F720 (also known as Color Guard) tough rubber coating. Between coatings of Color Guard, Kevlar® sheets (two layers each 0.61 mm thick) were laminated to the Color Guard along the side and top and bottom of the can. Kevlar® was necessary to prevent material from protruding through the can being subjected to external pressure. Because Kevlar® has virtually no compressive strength, it was deemed an acceptable jacket material for hydrostatic and triaxial testing where virtually all strains are compressive when compared to the initial geometry of the sample. Four balloons were then placed around each sample and sealed with Color Guard near the nipple flange interface on the top of the can. The Kevlar® sheets and balloons are shown in Figure 4. For the final two ¼-scale hydrostatic tests and most of the triaxial tests, the balloons were replaced with PMC®-770 urethane rubber (Figure 5) as it was felt this would maintain a better seal at the nipple protrusion. Lower

confining pressure triaxial tests were initially only coated with PMC®-770 urethane rubber, but after major breaches in the side of the sample occurred, all remaining triaxial tests were jacketed the same as the final two hydrostatic tests and occasionally additional balloons were added over the Color Guard/Kevlar®/PMC®-770 jacket.

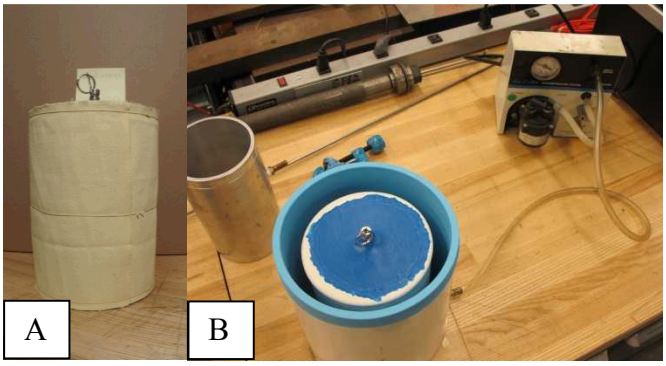

Fig. 4. A) ¼-scale hydrostatic sample showing Kevlar® sheets wrapped around Color Guard coated sample and B) method of balloon installation using vacuum pump.

Fig. 5. Hydrostatic sample (¼-scale) being coated with PMC®-770 urethane rubber over the three coats of Color Guard and two layers of Kevlar® sheets.

Hydrostatic full-scale samples were jacketed in a similar manner to the ¼-scale samples where a combination of Kevlar® and rubber coating were applied. Where the full scale jackets differ from ¼-scale is the order of application. As shown in Figure 6, Kevlar® is first placed onto the sample. PMC®-770 is then brushed on so the Kevlar stays adhered to the drum. A product made by Smooth-On called Brush-On®40 is then brushed on with multiple coats over the Kevlar®.

Fig. 6. Full scale Hydrostatic sample with no jacket on left, wrapped with Kevlar® and one coat of PMC®-770 center and multiple coats of Brush-On®40 right.

The nomenclature for tests in the current study is as follows where Waste Compaction is WC, Hydrostatic Compaction is HC, Uniaxial Compaction is UC, Triaxial Compaction is TX, Non-Degraded Quarter-Scale is NDQ, Non-Degraded Full is NDF and ## is the respective sample number (for example, 01 and 02 for first and second samples). For triaxial samples the first two numbers indicate the confining pressure (CP) and then the respective sample number is listed by ##.

- ¼-scale hydrostatic: WC-HC-NDQ-##
- ¼-scale uniaxial: WC-UC-NDQ-##
- ¼-scale triaxial: WC-TX-NDQ-CP-##
- Full-scale hydrostatic: WC-HC-NDF-##
- Full-scale uniaxial: WC-UC-NDF-##

3. EXPERIMENTAL METHODS/EQUIPMENT

3.1 Hydrostatic Tests

Full scale hydrostatic test were conducted at Southwest Research Institute (SwRI) in the Marine Engineering Department and not at Sandia National Laboratories because of the requirements for a pressure vessel large enough to house a 55 gallon drum (Orlowski, 2015). All other tests were conducted at Sandia National Laboratories Geomechanics laboratory. Full scale hydrostatic tests used a spirometer for volume strain measurements. The spirometer measured air escaping the sample which directly correlated to a change in volume of the sample. Critical to accurate spirometer readings is the vent line not being clogged by can ingredients during the test. To aid in maintaining an unclogged vent line, a "T" fitting with filter material on either side was threaded onto the inside bung hole on the lid. The spirometer needed to be restroked multiple times during

a test due to the volume of air exiting the 55 gallon drum exceeding the capacity of the spirometer. When a spirometer restroke was needed, the test was paused and the airline to the sample valved off. After restroking the spirometer and making appropriate notes regarding the pre- and post-restroke position of the spirometer, the test was resumed. Figure 7 shows the pressure vessel used at SwRI along with the spirometer and signal conditioning system for the spirometer Linear Variable Differential Transformer (LVDT). Confining fluid for full scale hydrostatic tests was water. At multiple points during compaction, unload/reload cycles were performed to measure bulk modulus as a function of density for both full- and ¼-scale hydrostatic tests.

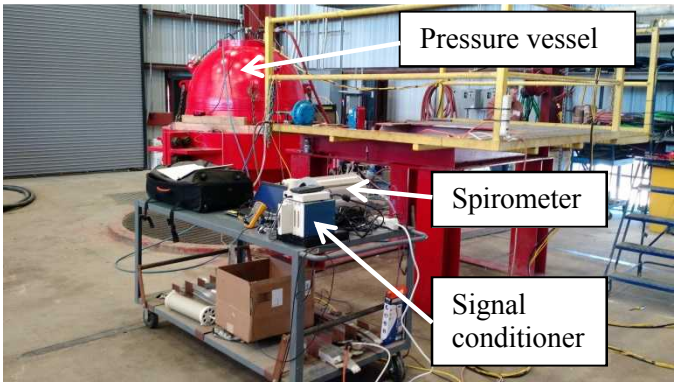

Fig. 7. Experimental setup at SwRI for full scale hydrostatic tests.

Volume strain was determined with the same spirometer for one ¼-scale hydrostatic test. The remaining ¼-scale hydrostatic tests used a flow meter. The flow meters used in this study are made by Alicat Scientific and are the Whisper Series where a very low pressure drop across the flow meter is required to record flow rate. The low pressure drop was required because if pressure was allowed to build up, the air inside the sample would compress and could give an inaccurate real time reading of air volume leaving the sample. Figure 8 shows the spirometer connected to the pressure vessel used for ¼-scale hydrostatic tests. Because of high volume strain of the samples, a large hydraulic piston was procured (Figure 9) to enable restroke free pressurization. This piston was used in our 5 MN load frame (Figure 10) to generate up to 15 MPa confining pressure in our 100 MPa pressure vessel.

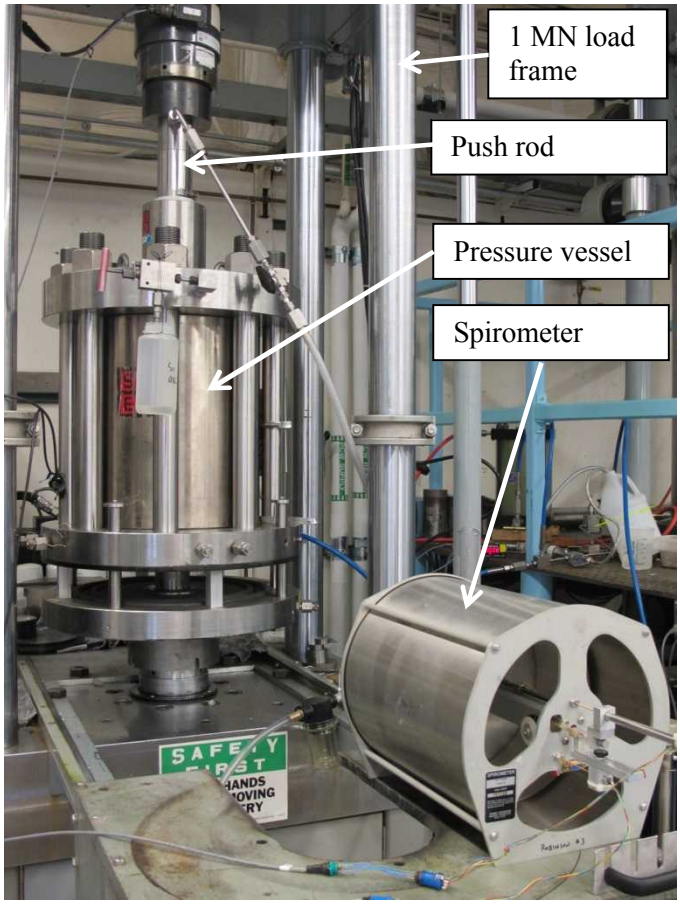

Fig. 8. Experimental setup for ¼-scale hydrostatic tests. The pressure vessel is large enough to house ¼-scale samples.

Fig. 9. High volume hydraulic piston used to generate hydrostatic pressure for ¼-scale tests. The piston was selected to eliminate restroking during pressurization.

3.2 Uniaxial Tests

Both full-scale and ¼-scale uniaxial tests were conducted at Sandia National Laboratories Geomechanics laboratory. Shown in Figure 10, full- and ¼-scale uniaxial tests utilized 5 MN and 1 MN load

frames respectively to achieve a target axial stress of 14.5 MPa. All three principal stresses and strains were recorded. Axial stress was measured from the load frame load cell; the other two principal stresses in uniaxial loading are zero. Axial strain was measured using the load frame LVDT and volume strain was measured from the air volume change of the sample and recorded using either the spirometer shown in Figure 8 or a flow meter. Bulk lateral strain was calculated from axial and volume strain components. During both full- and ¼-scale uniaxial tests, multiple crosshead resets were needed to accommodate large axial deformation of the samples. A correction that accounts for frame stretch at different crosshead heights was subtracted from recorded axial LVDT readings to isolate axial deformation of the sample from that of the load frame. At multiple points during compaction, unload/reload cycles were performed to measure elastic properties as a function of density.

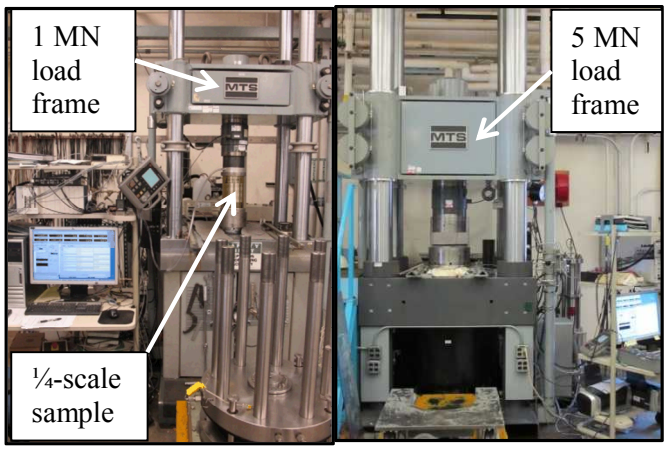

Fig. 10. 1 MN and 5 MN load frames used for testing of ¼-scale and full-scale uniaxial samples.

3.3 Triaxial Tests

Only ¼-scale triaxial tests were performed and all were tested using the 1 MN load frame with 100 MPa pressure vessel shown in Figure 8 (the spirometer was not used, but rather a flow meter for volume change measurements). The hydraulic piston shown in Figure 9 applied and maintained confining pressure and was actuated by the 5 MN load frame. Initially, a sample mounted LVDT for axial deformation measurement was used. Because of large axial deformation required and the strong correlation of the sample mounted LVDT compared to the corrected 1 MN frame LVDT, subsequent tests relied solely on the load frame LVDT. A triaxial sample was tested with the following steps:

- Perform a monotonic (no unload/reload loops) hydrostatic test to 1, 2, 5, or 15 MPa.
- Attach vent port with flexible metal tubing onto vent nipple on top of sample (Figure 11)
- Place compacted sample with vent port into an acrylic mold and form endcaps using Hydro-Stone® gypsum cement (Figure 11)
- Place sample with formed endcaps onto steel endcap inside 100 MPa pressure vessel
- Place second steel endcap on top of sample and assemble pressure vessel (Figure 11)
- Apply confining pressure equal to the hydrostatic pressure in the first step
- Advance 1 MN load frame actuator and perform unload/reload loops to measure elastic properties as a function of density

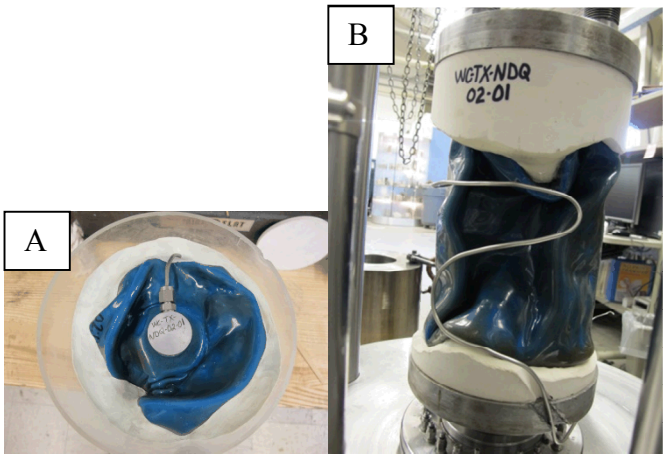

Fig. 11. Typical preparation for a triaxial test specimen: A) pre-compacted sample in acrylic mold with vent port added (white material is clay used to support pouring of Hydro-Stone® end cap) and B) sample assembly on base of 100 MPa pressure vessel showing end caps and flexible vent line.

3.4 Summary of Test Systems

Two computer-controlled servohydraulic test systems, manufactured by MTS Systems Corporation (MTS), were used in the testing of all ¼-scale and uniaxial full-scale samples. Full-scale hydrostatic samples were tested at SwRI in San Antonio, Texas. The systems were selected primarily to match capabilities to the load and confining pressure requirements specified in the test matrix. As shown in Table 2, the primary differences among the test systems were the maximum axial loads and confining pressures that could be applied during a test.

Triaxial, uniaxial, and hydrostatic ¼-scale tests were performed using our MTS 1.0 MN test system (Figure 10). This system was used in conjunction with our 100 MPa pressure vessel (Figure 8) and the high volume hydraulic piston (Figure 9) mounted in the 5 MN load frame for tests requiring pressurization. Uniaxial full scale tests were performed using the MTS 5.0 MN system also shown in Figure 10. Hydrostatic full scale tests used the SwRI pressure vessel shown in Figure 7.

The standard MTS four-column load frames used in this test series are equipped with movable crossheads to accommodate different specimen/equipment geometries. A hydraulic actuator located in the base of the frame is capable of applying axial force over the ranges specified in Table 2 in compression. Force is measured by an electronic load cell mounted on the crosshead; the relative displacement of the load actuator is determined from a LVDT mounted internal to the actuator housing.

Table 2: Test System Capabilities and Utilization

Test System	Axial Force Range MN (kip)	Confining Pressure Range MPa (ksi)	Utilization
SwRI pressure vessel (1.27 m ID)	NA	0 – 41.4 (0– 6)	Full scale hydrostatic
1.0 MN	0 – 1 (0 – 220)	0 – 100 (0 – 15)	¼-scale hydrostatic and triaxial samples tested with a 100 MPa pressure vessel. ¼-scale uniaxial
5.0 MN	0 – 5 (0 – 1000)	NA	Full-scale uniaxial and ¼-scale hydrostatic pressurization

4. TEST METHODS

4.1 Hydrostatic Tests

In practice there are several tasks that are critical to the overall test process in order to produce reliable and accurate measurements. When filling the pressure vessel, it is imperative to leave at least one port on top of the pressure vessel open to the atmosphere because initially the drum compacts substantially with very little pressure. At SwRI, this involved using a dipstick to constantly check water level in the pressure vessel during filling. When it was determined the pressure vessel was nearly full, the water valve was adjusted to substantially slow the rate of filling. Once water was observed from the vent port on top of the pressure vessel, the source valve was closed and water was allowed to stop flowing before the vent port was plugged. During the filling process, spirometer readings were monitored in case of premature drum crush.

A similar method was used on ¼-scale samples. Shop air was used to pressurize a reservoir filled with silicon oil. The shop air was set to approximately 5 psi and the top valve on the pressure vessel was left open. When fluid was observed exiting the top valve, the shop air was disconnected and once fluid stopped the top valve was closed. These settings prevented premature can crush during filling on the ¼-scale samples.

Full-scale hydrostatic tests were pressurized using two Haskel brand air pumps. The first air pump provided a volume strain of approximately 1E-4 sec^{-1}. When volume strain was approximately 50%, a larger air pump was used to apply a nearly constant pressure rate of 1.5 psi/sec. During pressurization, unload/reload pressure loops were performed at the intervals given in Table 3. Values in gray are target values and approximate values are what was observed on average for ¼-scale and full-scale samples at the target values. Following the pressurization rates above, pressurization time was approximately 300 minutes for ¼-scale and full scale tests.

Table 3: Criteria for performing an unload/reload loop for hydrostatic tests.

Volume strain	Confining Pressure MPa (psi)
0.12	~ 0.07 (10)
0.24	~ 0.10 (15)
0.36	~0.21 (30)
~0.39	0.34 (50)
~0.47	0.69 (100)
~0.53	1.38 (200)
~0.58	2.76 (400)
~0.61	5.52 (800)
~0.65	10.34 (1500)
~0.67	15.00 (2175)

A premature leak of a full scale drum prompted an investigation of the failure mode. From visual observation of a shakedown test and the current test, the deformed drums appeared to consistently collapse on three planes and if the vent bung happened to be in the middle of one of the planes, compaction near the lid had a tendency to push the bung out of the lid and thus create a leak in the sample (Figure 13). In order to force the bung to be located within the shaded circular region in Figure 13, three induced buckling points were created on the next sample. The desired buckling points in Figure 14 are shown with arrows on the top lid of the sample. A gentle tap with a rubber mallet created a slight dent at three points on the sample coinciding with the arrows drawn on the lid (one dent is shown). There was concern the initial buckling pressure during the test would be adversely affected but it proved to be nearly the same as a non-pre-induced buckled sample. Therefore the pre induced buckling technique was used on all remaining tests.

Pressure versus volume strain plots for ¼-scale and full-scale hydrostatic tests are shown in Figure 12. The ¼-scale plot went to target pressure of 15 MPa; no full-

scale test achieved the target pressure and the plot shown in Figure 12 is the sample that went to the highest pressure. The inset plots in Figure 12 are zoomed in to show the comparison of initial buckling pressure and subsequent sample crush up. The somewhat jagged response between unload/reload loops for the full-scale test is a result of restroking the spirometer multiple times.

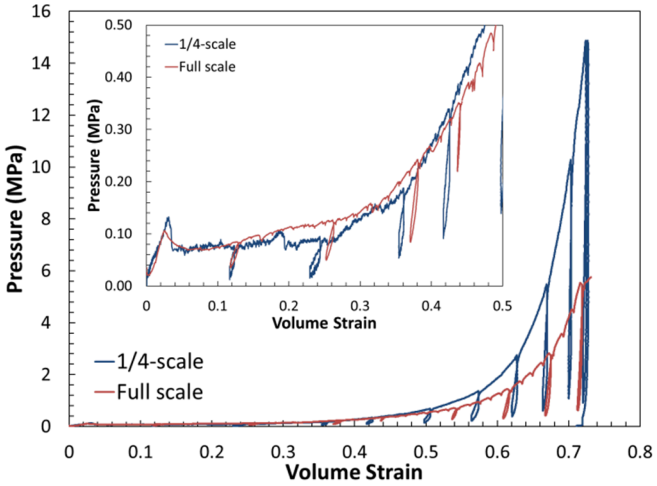

Fig. 12. Comparison of Pressure versus volume strain response for ¼-scale and full-scale hydrostatic tests.

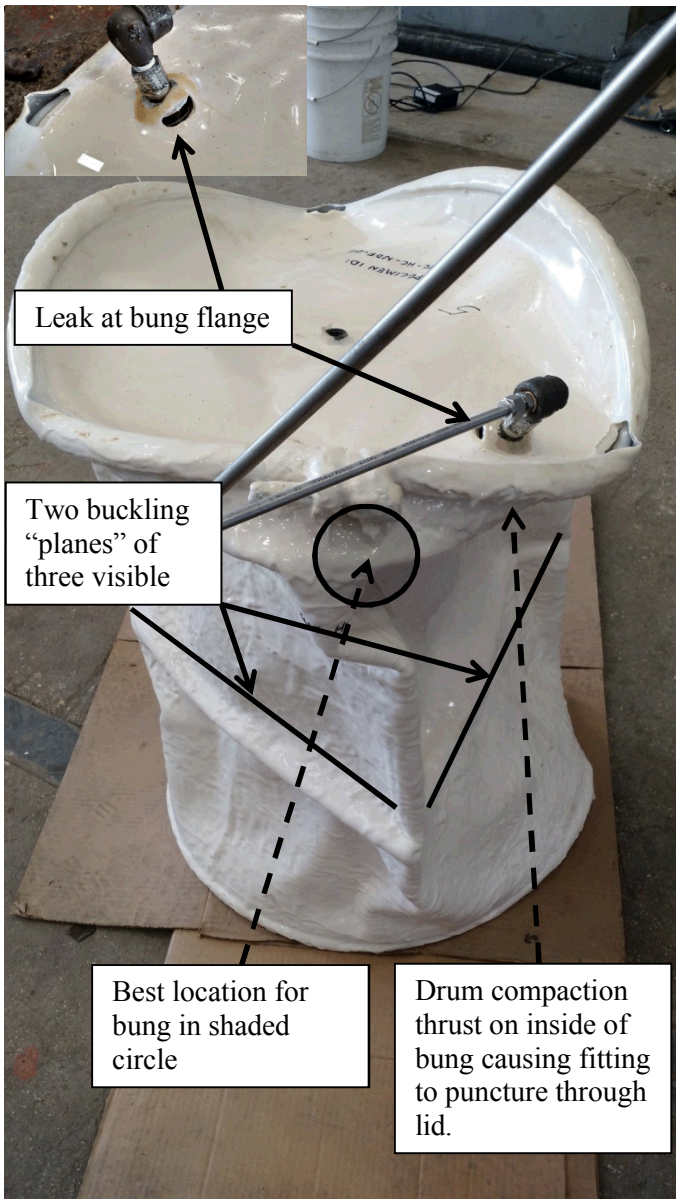

Fig. 13. Illustration of premature failure on a full-scale hydrostatic sample.

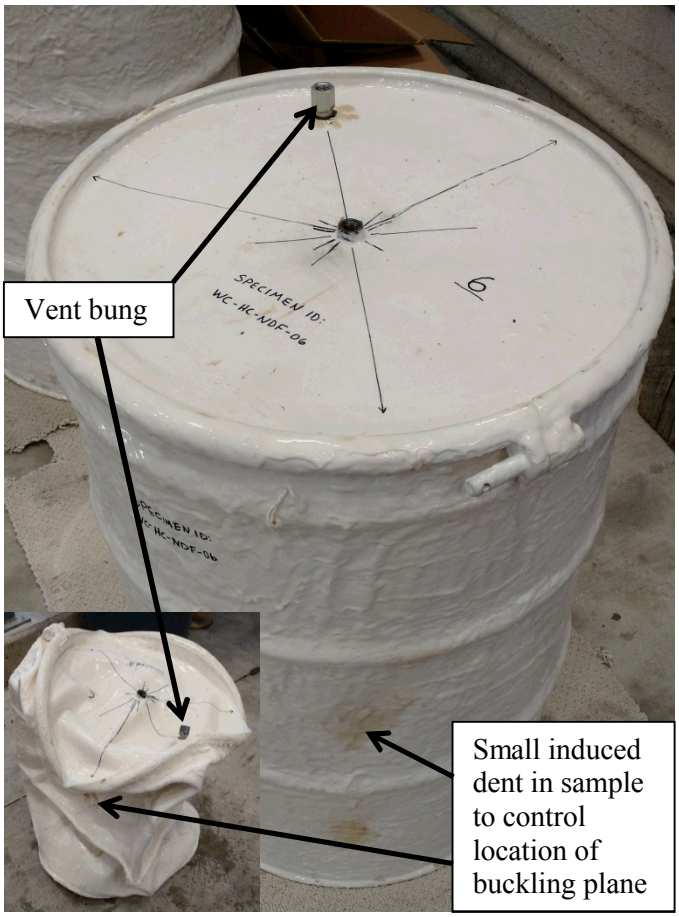

Fig. 14. Full-scale hydrostatic sample was tapped with a rubber mallet to induce a small dent which controlled the location of the buckling planes on the sample. The vent bung was then located at the junction of two buckling planes.

4.2 Uniaxial Tests

Although simpler to perform than hydrostatic and triaxial tests, uniaxial tests had their own difficulties. A jacket was used (PMC®-770) for full-scale samples that proved successful. Because the common breach mode for the ¼-scale uniaxial test was the side of the sample splitting open, it was decided to begin ¼-scale tests with no jacket and then when the load frame cross head needed to be reset and the test was paused, pack clay around the sample and then roll a balloon over the clay (Figure 2). For breaches along the side of the sample (Figure 15), the clay method worked well because the clay and balloon did not add significant tensile strength. Urethane rubber worked better for full scale tests because it remained intact across small holes in the sample (only one full scale sample split along the side and that one did so along the seam). Unload/reload loops were performed (eight or nine per test) so that at least three loops were accomplished during sample crush up and five loops during the region of significant stress increase. The unload/reload loops along with the entire stress versus strain curve (including zoomed in detail of axial strain during sample crush up) for a representative sample of each uniaxial test scale is shown in Figure 16.

All uniaxial tests were conducted at an axial strain rate of 1E-4 sec^{-1}.

Fig. 15. Typical post-test ¼-scale sample showing split along side of sample. White material around sample is clay used to seal the breaches in sample during testing. Full-scale uniaxial samples did not typically split but rather developed pinholes leaks.

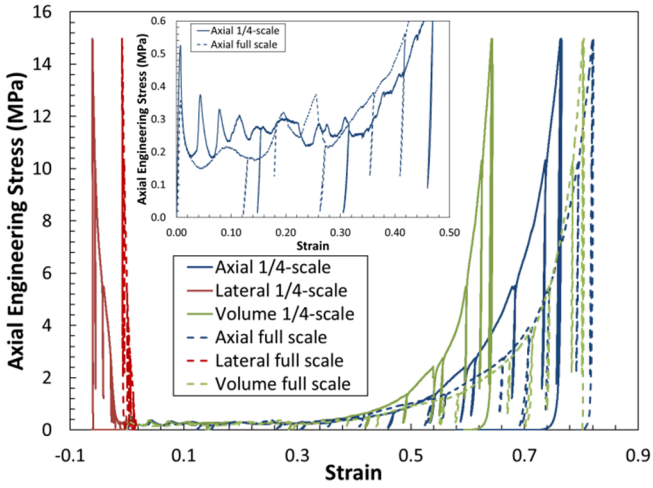

Fig. 16. Comparison of stress versus strain response for ¼-scale and full-scale uniaxial tests.

Whereas Figures 12 and 16 graphically show a comparison between ¼-scale and full-scale hydrostatic and uniaxial testing, Figure 17 shows a picture of representative samples of each configuration post-test. Note the similarity of compaction modes between ¼- and full-scale testing, as well as the different jacket material used for each test type.

Fig. 17. Comparison of full-scale and ¼-scale hydrostatic (left) and uniaxial samples (right). Note different jacket material used for each test configuration.

4.3 Triaxial Tests

A pilot triaxial test was performed on a tested hydrostatic sample. It proved difficult to produce higher pressure hydrostatic samples (5 and 15 MPa) for triaxial tests due to material puncturing through the sample and jacket material. To reduce jacket failure rate, triaxial samples were pre-compacted monotonically (i.e. no unload/reload loops) to the target confining pressure. The sample height was then measured and used for axial strain calculations during data reduction. Once sample endcaps were formed with Hydro-Stone® as described in Section 3.3 and shown in Figure 11, the sample was placed into the 100 MPa pressure vessel shown in Figure 8. Confining pressure was increased to match the pre-compaction pressure and held constant while the 1 MN load frame actuator was displaced at a strain rate of 1E-4 sec^{-1} to apply axial differential stress.

Unload/reload loops were not as systematic as with hydrostatic and uniaxial tests with the reason being it was unknown what value differential stress would achieve before a breach in the sample jacket and the desire was to achieve as much axial strain/stress as possible. The minimum number of differential stress unload/reload loops was two on a 5 MPa triaxial sample and the maximum number of loops was nine on a 2 MPa sample. Differential stress versus strain is plotted for the aforementioned 2 MPa triaxial sample in Figure 18. At 35% axial strain, this test achieved the highest axial strain of all triaxial tests. The least amount of axial strain (approximately 6%) before a jacket breach was from the 5 MPa triaxial sample where only two unload/reload loops were performed prior to failure of the sample. To illustrate the high volume strain during hydrostatic pre-compaction and then subsequent high axial strain during triaxial compaction, Figure 19 shows an undeformed sample, then post-hydrostatic compaction to 15 MPa, and finally post-triaxial compaction achieving a differential stress over 20 MPa.

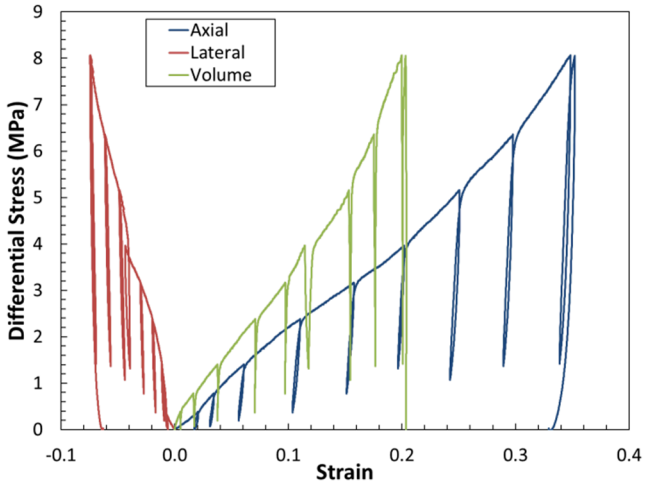

Fig. 18. Differential stress versus strain for a 2 MPa confining stress triaxial sample. This test achieved the highest axial strain of all triaxial tests.

Fig. 19. From left to right: 15 MPa pretest sample, post 15 MPa hydrostatic compaction ready for triaxial testing, and post 27% axial strain after triaxial compaction.

5. DATA REDUCTION

Data obtained from the data acquisition system (DAS) during each test included axial force, confining pressure, axial displacement, air volume (from flow meters or spirometer), and elapsed time. All data were collected in voltage form. These data were transferred to individual Microsoft® Excel spreadsheets where they were converted to engineering units of stress and strain which were subsequently plotted in graphical form for visual display and analysis.

During this data reduction, the traditional rock mechanics sign convention was used in which compressive stresses and strains are taken as positive quantities and tensile stresses and strains are taken as negative quantities.

All test types except for full-scale hydrostatic utilized a flow meter for volume change measurements. The flow meter signal was recorded in voltage form and when the calibrated sensitivity value was applied, the units were volume per unit time (cc/min). In order to efficiently convert the data to volume, the data was integrated using the "cumtrapz" function in Matlab®. The "trapz" function uses trapezoidal numerical integration with unit spacing.

5.1 Hydrostatic Tests

Data was collected from all hydrostatic compression tests to facilitate creation of pressure versus volumetric strain plots. Pressure is collected directly from the DAS in voltage form and converted to pressure units (MPa) using calibration sensitivity values. Volume was determined by measuring (in voltage) either the flow meter output or position of the spirometer (using the spirometer LVDT) and converting to units of volume using calibration sensitivity values, the area of the spirometer, and integration using Matlab® as described above.

Bulk modulus values as a function of confining pressure, volume strain, and sample density were determined for both ¼-scale and full-scale samples. Bulk modulus was calculated from,

$$K = \frac{\sigma_c}{\varepsilon_v} \tag{1}$$

where σ_c is confining pressure and ε_v is volumetric strain.

5.2 Triaxial Tests

Data was collected from all triaxial compression tests to facilitate creation of differential stress versus axial, lateral, and volume strain plots. Specifically, the data collected were time, confining pressure, axial force, axial sample displacement and/or load frame displacement, and changes in volume. Lateral strain, ε_l, was calculated from,

$$\varepsilon_l = \frac{(\varepsilon_v - \varepsilon_a)}{2} \tag{2}$$

where ε_v is volume strain and ε_a is axial strain.

Starting post-hydrostatic compaction length, area, and volume were necessary values to ensure stress and strains were calculated as accurately as possible. After hydrostatic compaction, the sample length and volume were determined; the length established from physically measuring the average height of the deformed sample and the volume change determined from the flow meter or spirometer data. Sample area was then determined from the volume divided by the length. Differential stress was then calculated from,

$$\sigma_D = \frac{F_{sp}^a}{\frac{\pi}{4}\left(D_{sp}^0\right)^2} \tag{3}$$

and axial strain and volume strain were calculated from,

$$\varepsilon_a = \left(\frac{\Delta L_{sp}}{L_{sp}^o}\right) \tag{4}$$

$$\varepsilon_v = \left(\frac{\Delta V_{sp}}{V_{sp}^o}\right) \tag{5}$$

where:

F_{sp}^a	=	Axial specimen force
D_{sp}^o	=	Original specimen diameter
ΔL_{sp}	=	Change in specimen length
L_{sp}^o	=	Original specimen length
ΔV_{sp}	=	Change in specimen volume
$V^o{}_{sp}$	=	Original specimen volume

Because axial displacement was recorded using the load frame LVDT for most triaxial tests, a correction was applied to factor out the stiffness of the load frame. The 1 MN load frame was cycled with the crosshead in a similar position to that when a triaxial test was being conducted. A best fit linear regression was applied to the data set (Figure 20). Then for each recorded value of displacement, the equation of the line was subtracted using the corresponding force value in place of "x" in the equation.

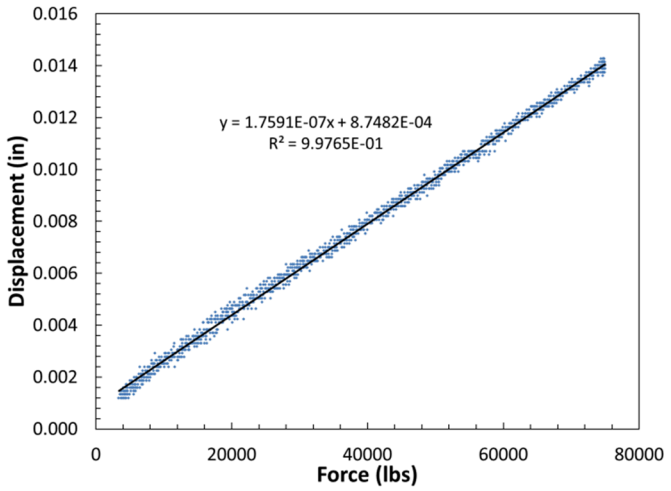

Fig. 20. 1 MN load frame stiffness with crosshead in similar position for triaxial testing. The equation of the line is used to factor out the stretch of the load frame for a given force value.

5.3 Uniaxial Tests

Data was collected from all uniaxial compression tests to facilitate creation of an axial stress versus axial, lateral, and volume strain plot. Specifically, the data collected were time, axial force, load frame displacement, and volumetric changes. Lateral strain, ε_l, was calculated from Eq 2.

Axial stress, and axial and volume strain were determined from Eqs. 3, 4, and 5. As discussed in the triaxial section, uniaxial ¼-scale tests used the same correction for axial displacement as shown in Figure 20. Full scale uniaxial tests used the correction shown in Figure 21 for the 5 MN load frame.

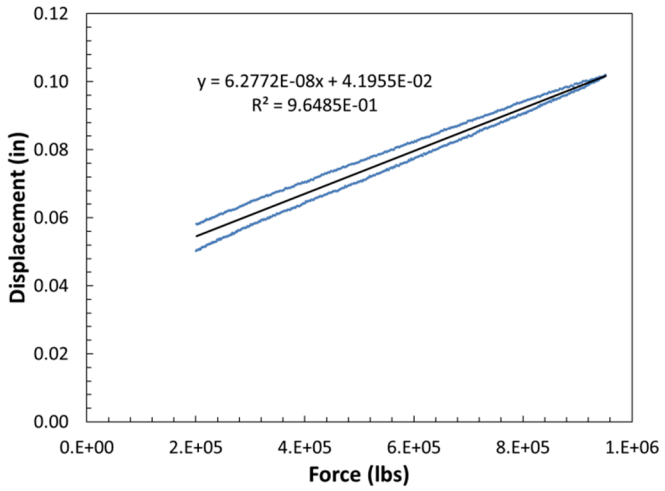

Fig. 21. 5 MN load frame stiffness with crosshead in lowest position of uniaxial test. The equation of the line is used to factor out the stretch of the load frame for a given force value.

For full-scale uniaxial tests, compensation in the stiffness correction for different load frame column post exposed lengths (i.e. crosshead being reset multiple times during one test) was factored into the correction by knowing the cross sectional area, Young's modulus of the four posts on the 5 MN load frame, and the current force.

6. RESULTS

6.1 Hydrostatic Tests

A total of eight hydrostatic tests were performed, four each on the ¼-scale and full-scale samples. That the results were consistent from sample to sample was apparent by both post-test observation and from the pressure versus volume responses. Figure 22 shows all post-test hydrostatic samples of both ¼-scale and full-scale. Note that WC-HC-NDQ-02 is shorter because that sample was used for a triaxial test.

Table 4 lists the final density of all hydrostatic tests and gives the pressure of jacket breach or blocking of the vent port. Note that only one hydrostatic sample (WC-HC-NDQ-02) did not leak or develop a clogged vent port.

Fig. 22. Posttest ¼-scale (A) and full-scale (B) hydrostatic compression samples. Samples in numerical order from left to right.

Combined pressure versus volume strain response of all hydrostatic samples is shown in Figure 23 and illustrates the consistency between scales and within groups of ¼-scale and full-scale samples. Full-scale hydrostatic samples achieved higher volume strain for a given pressure than ¼-scale. Sample WC-HC-NDF-01 leaked causing increasing volume strain without an increase in pressure. The vent ports for samples WC-HC-NDQ-03 and WC-HC-NDQ-04 clogged at 10.3 and 2.7 MPa confining pressure resulting in an increase in pressure without an increase in volume strain.

Bulk modulus plotted versus density for all hydrostatic tests is shown in graphical form in Figure 24. Bulk modulus is calculated from either two points or the most linear region during unloading from the unload/reload loop. For the two point method, the upper point is where the reload data intersects the unload data and the lower point is the lowest pressure measured during unloading. Using these two points effectively averages the slope of the u/r loop.

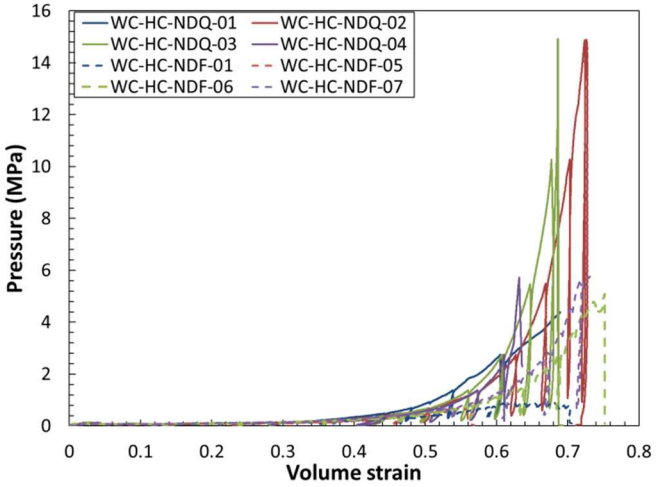

Fig. 23. Pressure versus volume strain for all hydrostatic samples.

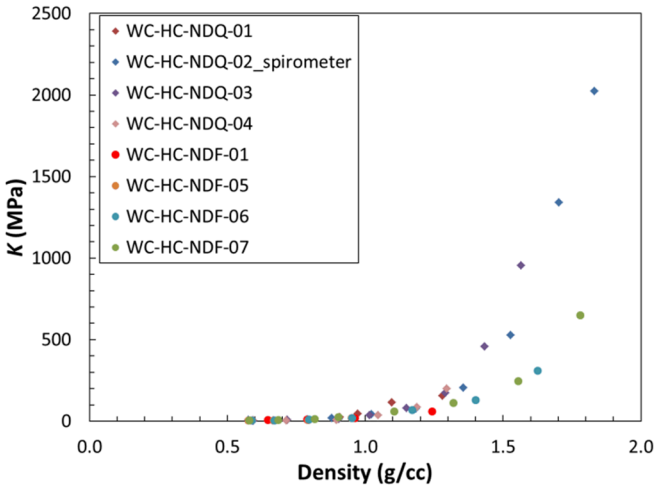

Fig. 24. Bulk modulus versus density for all hydrostatic tests.

Table 4: Density values for all hydrostatic samples.

Sample	¼ or Full Scale	Post-test Density* (g/cc)	Comments
WC-HC-NDQ-01	1/4	1.28	Density at 2.7 MPa and leak at 4.4 MPa
WC-HC-NDQ-02	1/4	1.83	Density at 14.9 MPa
WC-HC-NDQ-03	1/4	1.57	Density and clogged vent at 10.3 MPa
WC-HC-NDQ-04	1/4	1.3	Density and clogged vent at 2.7 MPa
WC-HC-NDF-01	Full	1.2	Density at 0.7 MPa and leak at 0.8 MPa
WC-HC-NDF-05	Full	1.0	Density at 0.3 MPa and leak at 0.7 MPa
WC-HC-NDF-06	Full	1.6	Density at 2.7 MPa and leak at 5.0 MPa
WC-HC-NDF-07	Full	1.8	Density at 5.5 MPa and leak at 5.8 MPa
* Pre-test density for all samples was 0.5055 g/cc * Post-test density reflects density when last unload/reload loop was performed which was usually near the end of test			

6.2 Triaxial Tests

Seven triaxial tests were performed on ¼-scale samples. The first test performed (WC-TX-NDQ-10-01) was targeted for testing at 15 MPa confining pressure but developed a leak around 10 MPa and thus no data is provided for this sample. No triaxial tests were conducted on full scale drums. Test confining pressures were 1, 2, 5, and 15 MPa.

Based on axial and volume change measurements of each sample after hydrostatic compaction to target triaxial confining pressure, Table 5 lists the density for each triaxial sample at two different stages during the test: 1) post hydrostatic compaction, and 2) post final unload/reload loop. The initial density (pre hydrostatic) for all samples was 0.5055 g/cc. The final unload/reload loop was performed close to the end of the test as unload/reload loops were performed at frequent intervals until a breach of confining fluid inside the sample. Note how post hydrostatic densities are ordered from greatest to least following hydrostatic compaction pressures, and for tests at the same confining pressure, the densities match.

Elastic properties as a function of density are represented graphically in Figure 25. Albeit with some scatter for test WC-TX-NDQ-15-02, Young's modulus, calculated as the slope of the differential stress versus axial strain unload/reload loop, generally increases with increasing density. Poisson's ratio was calculated from,

$$\nu = \left(\frac{E}{\sigma_D / \varepsilon_L} \right) \tag{6}$$

where:

E = Young's modulus

σ_D = Differential stress

ε_L = Lateral strain

Poisson's ratio ranges from 0.18 to 0.69. It is acknowledged that Poisson ratios for many materials are not possible over 0.5. However, we feel these numbers are real and are a result of:

- the irregular geometry of the samples
- reflect bulk lateral response of the sample
- some of the contents within the samples are fairly rigid and randomly distributed

Table 5: Density values all triaxial samples.

Sample	Density post hydrostatic compaction (g/cc)	Density post triax test (g/cc)
WC-TX-NDQ-15-02	1.66	2.69
WC-TX-NDQ-10-01	No test due to jacket leak	
WC-TX-NDQ-05-01	1.21	1.76
WC-TX-NDQ-02-03	1.09	1.47
WC-TX-NDQ-02-01	1.09	1.70
WC-TX-NDQ-01-03	1.02	1.30
WC-TX-NDQ-01-02	1.02	1.20

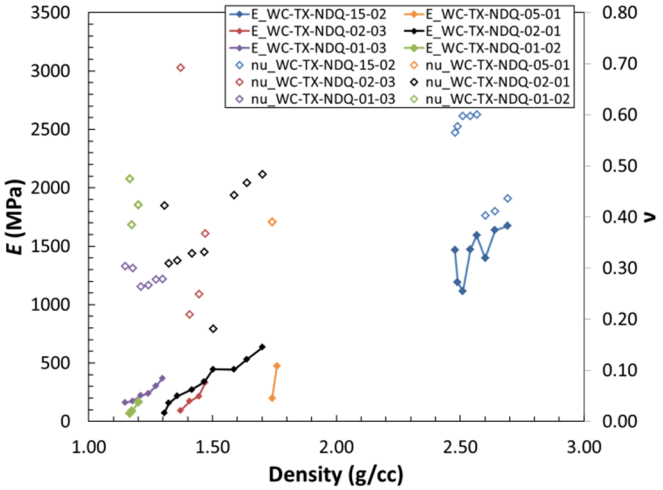

Fig. 25. Young's modulus and Poisson's ratio versus density for all triaxial tests.

6.3 Uniaxial tests

Nine uniaxial tests were conducted (five ¼-scale and four full-scale). Figure 16 shows typical axial stress versus strain curves where ¼-scale and full-scale are compared. Table 6 lists final densities and at what axial stress they were calculated. Samples WC-UC-NDQ-02 and WC-UC-NDF-03 split excessively along the side wall of the sample and the air tight seal of the sample was not obtainable. For these tests, only axial stress and strain data is valid up to target compaction stress of 15 MPa. Volume and therefore lateral strain must be discarded after the air tight seal of the sample was lost.

Table 6: Density values all uniaxial samples.

Sample	¼ or Full scale	Post-test Density* (g/cc)	Axial Stress (MPa)
WC-UC-NDQ-01	1/4	1.54	14.2
WC-UC-NDQ-02	1/4	1.17	5.5
WC-UC-NDQ-03	1/4	1.41	15.0
WC-UC-NDQ-04	1/4	1.53	15.0
WC-HC-NDQ-05	1/4	1.49	15.0
WC-UC-NDF-01	Full	2.55	16.8
WC-UC-NDF-02	Full	2.5	15.0
WC-UC-NDF-03	Full	1.48	2.8
WC-UC-NDF-04	Full	2.56	15.0

* Pre-test density for all samples was 0.5055 g/cc
* Final density measurement at the listed axial stress

Figure 26 plots Young's modulus and Poisson's ratio as a function of sample density. Young's modulus increases exponentially for both ¼-scale and full-scale samples. There is a large difference in the relationship of Young's moduli between the two sets of samples, i.e. for a given density, Young's modulus is much lower for full-scale samples. Poisson's ratio is between 0.05 and 0.25 for all recordings with one exception; sample WC-UC-NDQ-03 exhibited a negative Poisson's ratio at an axial stress of 2.4 MPa. While it could be argued this was a result of an anomalous piece of material thrusting inside the sample, it is more likely a measurement error and should be discounted.

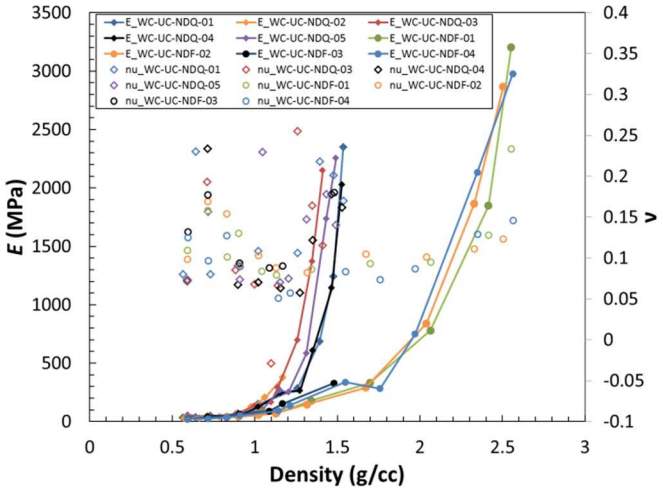

Fig. 26. Young's modulus and Poisson's ratio versus density for all uniaxial tests.

7. CONCLUSIONS

A test suite was conducted that established the following for ¼-and full-scale containers filled with WIPP surrogate waste using a recipe based on the analysis of Hansen et al (1997), modified to a starting test density from the CRA-2014 waste inventory:

- Bulk modulus was determined as a function of density from hydrostatic loading
- Young's modulus and Poisson's ratio were determined as a function of density from uniaxial loading
- Young's modulus and Poisson's ratio were determined as a function of density from triaxial loading

In some cases, novel test methods and equipment were developed to handle the unique material composition. Included were the following: 1) use of a spirometer capable of handling large volumetric strains while still giving the precision necessary for reliable bulk modulus measurements and 2) unique coating techniques that preserved the air tightness of the test samples and acted

as jackets during hydrostatic, triaxial and uniaxial testing.

This work was funded by DOE through WIPP programs.

Sandia National Laboratories is a multi-program laboratory managed and operated by Sandia Corporation, a wholly owned subsidiary of Lockheed Martin Corporation, for the U.S. Department of Energy's National Nuclear Security Administration under contract DE-AC04-94AL85000.

This research is funded by WIPP programs administered by the Office of Environmental Management (EM) of the U.S Department of Energy.

REFERENCES

Baker, W.E., Ransleven, G.E., Friesenhahn, G.J., and Hokanson, J.C., 1980, *A Review of Accident Simulation in Low-Level Nuclear Waste Transportation*, Report No. TTC-0054, Prepared for Sandia National Laboratories, Contract No. 13-6665, SwRI Project No. 136665, Southwest Research Institute, San Antonio, TX.

Butcher, B.M., Thompson, T.W., VanBuskirk, R.G., and Patti, N.C., 1991, *Mechanical Compaction of Waste Isolation Pilot Plant Simulated Waste*, Sandia Report SAND90-1206, Sandia National Laboratories, Albuquerque, NM.

Hansen, F.D., Knowles, M.K., Thompson, T.W., Gross, M., McLennan, J.D., Schatz, J.F., 1997. Description and Evaluation of a Mechanistically Based Conceptual Model for Spall, *SAND97-1369*, Sandia National Laboratories, Albuquerque, NM.

Huerta, M., Lamoreaux, G.H., Romesberg, L.E., Yoshimura, H.R., Joseph, B.J., May, R.A, 1983. Analysis, Scale Modeling, and Full-Scale Tests of Low-Level Nuclear Waste Drum Response to Accident Environments, *SAND80-2517*, Sandia National Laboratories, Albuquerque, NM.

Orlowski, M. 2015. WIPP Full Scale Hydrostatic Testing of 55 Gallon Waste Disposal Drums, Final Report, Issue 1. Prepared for Sandia National Laboratories, Carlsbad, NM. SwRI Project 18.18197.03. Southwest Research Institute, San Antonio, TX.

VandeKraats, J., 1987, *Quarter-Scale Modeling of Room Convergence Effects on CH TRU Drum Waste Emplacements Using WIPP Reference Design Geometries*, Report DOE/WIPP 87-012, Prepared for the Department of Energy under Contract DE-AC04-86AL31950, Westinghouse Experimental Engineering, Carlsbad, NM.

Wawersik, W. R., 2001, *One-Quarter-Scale Laboratory Crush Tests on Unconfined Waste Cans and a Confined Waste Package in Support of the Waste Isolation Pilot Plant (WIPP)*, Sandia Report SAND98-2574, Sandia National Laboratories, Albuquerque, NM.